Neuron, Vol. 15, 1203–1218, November, 1995, Copyright © 1995 by Cell Press

Age-Related CNS Disorder and Early Death in Transgenic FVB/N Mice Overexpressing Alzheimer Amyloid Precursor Proteins

Karen K. Hsiao,* David R. Borchelt,† Kristine Olson,* Rosa Johannsdottir,* Cheryl Kitt,† Wael Yunis,‡ Sherry Xu,* Chris Eckman,§ Steven Younkin,§ Donald Price,† Costantino Iadecola,* H. Brent Clark,*‡ and George Carlson‖

*Department of Neurology
‡Department of Laboratory Medicine and Pathology
University of Minnesota
Minneapolis, Minnesota 55455
†Department of Pathology
Johns Hopkins University
Baltimore, Maryland 21205
‖McLaughlin Research Institute
Great Falls, Montana 59405
§Mayo Clinic Jacksonville
Jacksonville, Florida 32224

Summary

Transgenic FVB/N mice overexpressing human (Hu) or mouse (Mo) Alzheimer amyloid precursor protein (APP_{695}) die early and develop a CNS disorder that includes neophobia and impaired spatial alternation, with diminished glucose utilization and astrogliosis mainly in the cerebrum. Age at onset of neophobia and age at death decrease with increasing levels of brain APP. HuAPP transgenes induce death much earlier than MoAPP transgenes expressed at similar levels. No extracellular amyloid was detected, indicating that some deleterious processes related to APP overexpression are dissociated from formation of amyloid. A similar clinical syndrome occurs spontaneously in ~20% of nontransgenic mice when they reach mid- to late-adult life, suggesting that APP overexpression may accelerate a naturally occuring age-related CNS disorder in FVB/N mice.

Introduction

Age and genes, either as specific alleles (e.g., ApoE4) or as mutants (e.g., amyloid precursor protein [APP] and S182), are the major risk factors for Alzheimer's disease (AD). Patients with AD exhibit to a greater degree abnormalities that are similar to those occurring in the brains of many nondemented elderly individuals, including amyloid deposits, neurofibrillary tangles, reductions in numbers of neurons and synapses in certain regions, and astrocytic gliosis (Crystal et al., 1988; Arriagada et al., 1992). The incidence of AD increases dramatically in late life, with as many as 47% of those over the age of 85 having AD (Evans et al., 1989; Kokmen et al., 1989). Because mild cognitive deficits and some of the histologic manifestations of AD are present in aged individuals without AD, there is speculation that similar processes may occur in both mildly impaired, aged individuals and cases of AD.

Genes on chromosomes 21, 19, 14, and 1 are associated with AD (Goate et al., 1991; Corder et al., 1993; Levy-Lehad et al., 1995; Sherrington et al., 1995). The APP gene on chromosome 21 encodes a transmembrane protein expressed in brain and other tissues, and five mutations in this gene can cause early onset familial AD (Chartier-Harlin et al., 1991; Goate et al., 1991; Murrell et al., 1991; Hendriks et al., 1992; Mullan et al., 1992). All five mutations occur within or near the β-amyloid (Aβ) domain, a 4 kDa fragment present in amyloid, and these mutations may influence APP processing to facilitate amyloid formation. In cultured cells, APP with the V717I mutation is associated with an increase in the $A\beta_{1-42}$ peptide (Suzuki et al., 1994), while APP with K670N–M671L, termed the Swedish mutation, is associated with increased $A\beta_{1-40}$ secretion (Citron et al., 1992; Cai et al., 1993). These results support the argument that events related to the processing of APP and the generation of Aβ underlie the CNS dysfunction in early onset familial AD. Patients with trisomy 21 (Down's syndrome) overexpress APP and develop AD-like pathology and cognitive decline, often before the fifth decade, indicating a role for APP overexpression. While the evidence supporting the involvement of APP and Aβ in AD is compelling, how these molecules are related to the neurologic dysfunction of AD remains controversial. To investigate the biologic effects of overexpression of APP with or without AD-linked mutations, we produced Tg mice expressing either wild-type or mutant APP. We reasoned that both wild-type and mutant APP might induce early neurologic dysfunction in Tg mice, since the presence of extra copies (Down's syndrome) or mutations (familial AD) is associated in humans with early onset AD–like pathology. Because the senescent changes that occur in many elderly individuals resemble sporadic AD, we also examined aged non-Tg mice.

FVB/N mice were chosen because they are an inbred strain with prominent pronuclei in single-cell embryos and high fertility, making them useful for transgenic approaches (Taketo et al., 1991). FVB/N mice are related to the Swiss stock. All Tg lines that overexpressed APP, whether mutant or wild type, died early and developed a neurologic syndrome similar to that seen in some aged FVB/N mice.

Results

PrP Cosmid Vector Drives Overexpression of APP in Transgenic Mice

To determine the effect of mutant and wild-type APP expression in FVB/N mice, we replaced the prion protein (PrP) open reading frame (ORF) with a variety of APP ORFs in a hamster PrP cosmid vector (Scott et al., 1992), which has been shown to drive position-independent, copy number–dependent transgene product expression in the brain (Scott et al., 1989; Prusiner et al., 1990; Westaway et al., 1994). Tg mice harbored one of four different

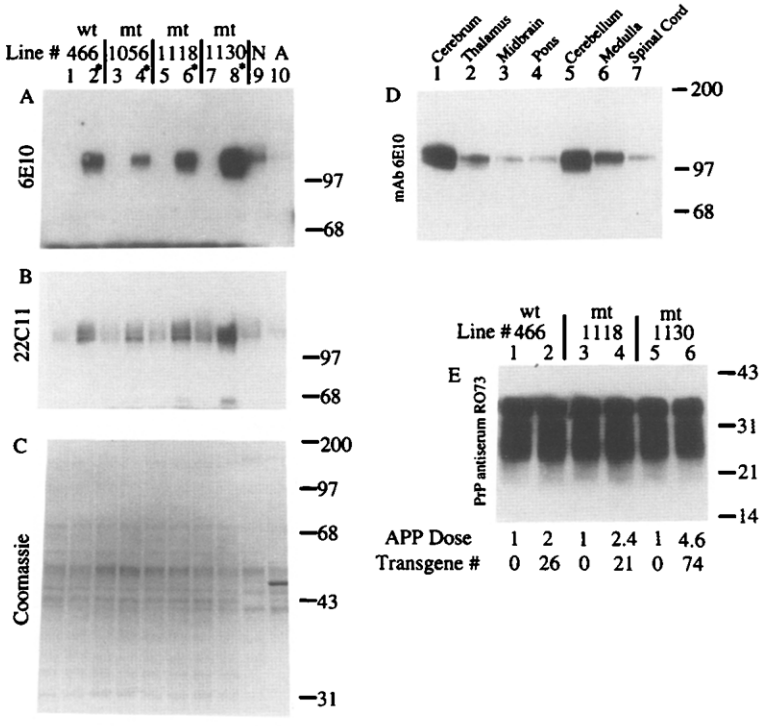

Figure 1. Transgenic APP Protein Expression in Brain Tissue

Transgenic APP protein expression was measured in a semiquantitative fashion in 4 lines of Tg mice, Tg(HuAPP$_{695}$.WTmyc)466, Tg (HuAPP$_{695}$.TRImyc)1056, Tg(HuAPP$_{695}$.TRImyc) 1118, and Tg(HuAPP$_{695}$.TRImyc)1130H, harboring 26, 7, 21, and 74 transgene copy numbers, respectively. Equivalent amounts of protein from detergent-extracted brain homogenates of non-Tg and Tg (asterisks) littermates were immunoblotted in parallel. Equivalent amounts of protein from detergent-extracted brain homogenates of normal human (lane 9) and AD (lane 10) brain were immunoblotted. Primary antibody was revealed by ^{125}I–protein A. For monoclonal antibodies, blots were first incubated with rabbit antiserum to mouse IgG. The amount of bound ^{125}I-protein A was quantified using a phosphorimager, demonstrating a direct relationship between transgene copy number and transgene product expression.

(A) To measure the level of HuAPP specifically, brain homogenates were probed with 6E10 antibody raised against residues 1–17 of human Aβ (Kim et al., 1990).

(B) Relative levels of transgenic compared with endogenous brain MoAPP were examined by immunoblot analysis with a monoclonal antibody, 22C11, which detects both HuAPP and MoAPP.

(C) Coomassie stain of protein in brain extracts shown to control for protein loading.

(D) The relative amount of HuAPP in 10% (w/v) homogenates of various brain regions was specifically detected in Tg(HuAPP$_{695}$.TRImyc)1130H mice using the 6E10 antibody, as described above. Equivalent amounts of protein were immunoblotted in each lane. The highest HuAPP level, in the cerebrum, was approximately twice that of the cerebellum.

(E) No difference in expression of PrP was found in 10% (w/v) homogenates of brain tissue from Tg mice harboring 21, 26, or 74 transgene copies and nontransgenic littermates using the antiserum R073.

transgenes, some containing mutations associated with familial AD (MoAPP$_{695}$.WT [wild type]; HuAPP$_{695}$.SWE [K670N and M671L, APP$_{770}$ numbering]; HuAPP$_{695}$.TRImyc [V717I, V721A, and M722V with a 3′-*myc* tag]; HuAPP$_{695}$.WTmyc [wild type with a 3′-*myc* tag]; Mo, Mouse; Hu, Human). Initially, we introduced transgenes with a 3′-*myc* tag, a 12 codon segment of the c-*myc* proto-oncogene, to facilitate immunodetection of transgene products (Wong and Cleveland, 1990). The *myc* tag exerted no apparent effect on the phenotype, since Tg(HuAPP$_{695}$.SWE) mice lacking the *myc* tag developed the same clinical and pathologic features. In later studies, the high level of APP expression obtained in our mice obviated the need for the *myc* tag. The experimental V721A and M722V mutations, unintentionally introduced to the APP ORF harboring the V717I mutation linked to early onset familial AD and discovered after Tg lines had been established, exerted no obvious effect on the phenotype since Tg(HuAPP$_{695}$.TRImyc) mice developed the same clinical and pathologic abnormalities as Tg mice expressing the other three transgenes. Subsequent analyses of HuAPP$_{695}$.TRImyc in cultured cells indicated that these unintentional mutations exert no significant effects on the processing of HuAPP relative to protein maturation, modification, or proteolytic processing to produce soluble ectodomains or Aβ peptides (D. R. B., G. Thinakaran, and S. Sisodia, unpublished data).

APP expression was measured in brains of Tg mice harboring different transgene copy numbers by quantitation of immunoblots in Tg lines with the monoclonal antibody 22C11 (Weidemann et al., 1989), which recognizes an identical epitope in both mouse and human APP (Figure 1B) as well as amyloid precursor–like protein 2 (APLP2), potentially leading to an underestimation of the amount of Tg APP relative to endogenous MoAPP (Slunt et al., 1994). APP protein expression in Tg brain depended upon copy number as well as the species of APP expressed (Figure 2). MoAPP transgenes achieved levels equivalent to those of HuAPP transgenes, but with fewer copies.

Measurement of Aβ in Tg(HuAPP$_{695}$.TRImyc) mice indicates that both Aβ$_{1-40}$ and Aβ$_{1-42}$ are generated in the brain (Table 1). Aβ levels were not measured in Tg FVB/N mice expressing HuAPP.SWE because of insufficient numbers of mice, owing to their poor breeding characteristics, and Aβ levels were not measured in Tg mice expressing MoAPP because methods for reliably measuring mouse Aβ in the brain are not yet available. The Ban50 capture antibody does not recognize MoAPP; levels indicated for non-Tg mice represent background signal. Both forms of Aβ were readily detectable in Tg mice but were significantly higher in lines overexpressing APP and exhibiting clinical abnormalities than in an unaffected line expressing lower levels of APP.

Specific immunostaining for human APP/Aβ using the

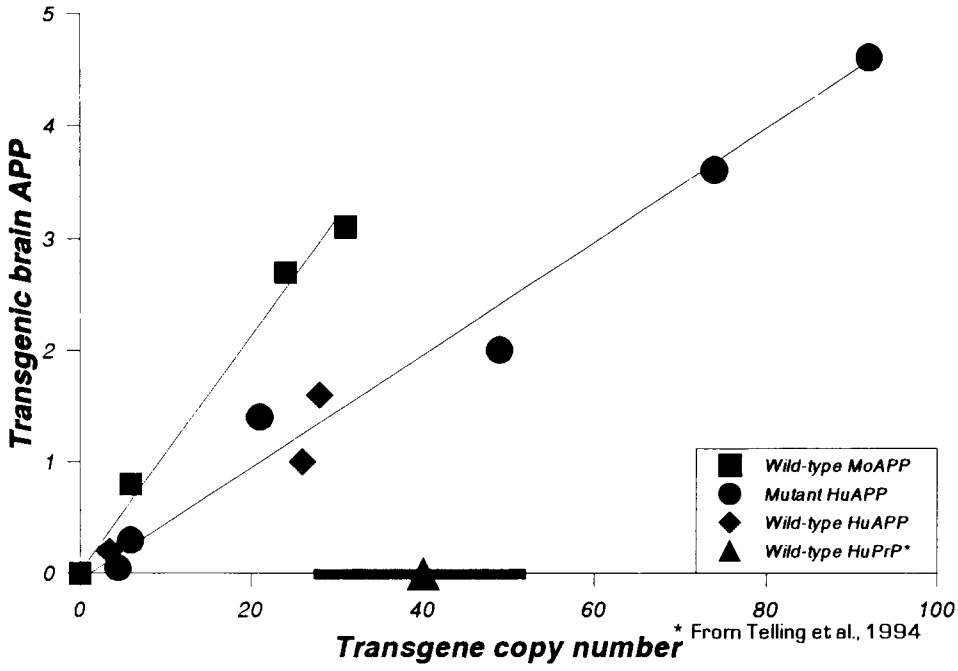

Figure 2. Dependence of Transgenic Brain APP Expression upon Transgene Species and Copy Number

Tg brain MoAPP (squares) and HuAPP (circles and diamonds) expression increases with rising transgene copy numbers. Total brain APP, detected with 22C11 antibody, was determined in 3 Tg mice from each line and 9 non-Tg age-matched mice. Tg brain APP was calculated by the ratio of total APP in Tg mice compared with non-Tg mice, minus 1. Both Tg HuAPP and Tg MoAPP were quantified by this method. MoAPP is more efficiently expressed than HuAPP. Nonspecific effects of the hamster PrP cosmid vector driving APP expression were not the cause of clinical abnormalities in Tg FVB/N mice overexpressing APP, since a previously published Tg line developed in FVB/N mice, Tg(HuPrP)FVB-152 (triangle), expressing human PrP driven by 30–50 copies of the hamster PrP gene cosmid exhibited no behavioral abnormalities or early death (Telling et al., 1994).

8E5 or 6E10 monoclonal antibodies revealed HuAPP in vescicular structures within large pyramidal cells of the hippocampus, parahippocampal area, amygdala, and cerebral cortex, as well as fainter staining throughout the brain in smaller neurons and some glial cells. Antibody 8E5 (gift of Dale Schenk, Athena Neurosciences) recognizes a segment of APP spanning residues 519–667 (APP_{770} numbering), and 6E10 recognizes residues 1–17 of human Aβ (Kim et al., 1990). The pattern of HuAPP immunostaining matched that of regional brain immunoblots showing the highest levels of expression in the cerebrum (see Figure 1D). The brain and spinal cord contained the highest levels of HuAPP; the striated muscle, heart, skin, and lung <5% of brain levels; and the thymus, liver, spleen, kidney, testes, and small intestine undetectable amounts (data not shown).

PrP levels remained unchanged in animals with high transgene copy numbers (see Figure 1E), indicating that the PrP promoter and other sequences in the transgenes did not deplete transcription factor pools, and that the cellular machinery for synthesizing, modifying, and translocating membrane glycoproteins was not overburdened.

Poor Reproductive Ability and Early Death in Tg FVB/N Mice Overexpressing APP

Of 19 founders identified, 7 failed to produce viable lines owing to death of the founder or poor fertility and short lifespan. FVB/N mice harboring >40 copies of the $HuAPP_{695}$.SWE transgene bred poorly and died within a year; only 1 of 5 founders produced offspring, Tg2123H. Tg2123H mice bred erratically, preventing full characterization of the line. Early clinical signs and death prevented

Table 1. Brain Aβ Levels in Transgenic Mice Expressing HuAPP.TRImyc

Level of Tg APP Expression	Animal Status	n	Age (days)	$Aβ_{1-40}$ (pmol/g)	$Aβ_{1-42}$ (pmol/g)
Non-Tg	Well[a]	11	81.1 ± 10.2	0.85 ± 0.36	0.18 ± 0.10
Low	Well	2	109	1.56	0.5
High	Well	3	34 ± 0	7.95 ± 0.96	4.74 ± 0.67
High	Affected[b]	4	93.3 ± 7.9	12.27 ± 1.07	3.23 ± 1.41

Animals with high levels of Tg APP expression were selected from Tg1130H and Tg1140, animals with low levels of Tg APP expression were selected from Tg1056. Where applicable, values are mean ± SEM.

[a] Corner index scores > 1.

[b] Animals failed corner index testing (two scores of "0" or a "0" and "1" in three consecutive testing sessions).

Table 2. Clinical and Pathological Features of FVB/N Mice Expressing APP Transgenes

Line[a]	Copy Number[b] (mean ± SEM)	Transgenic APP[c] (mean ± SEM)	100 Days of Age		Days of Age ± SEM				Cortico-Limbic Gliosis	Amyloid Deposits[g]
			% Neophobic[d] (N)	% Dead[e]	25% Dead	50% Dead	75% Dead	N (n)[f]		
Tg(HuAPP$_{695}$.SWE)2123H	46[h]	NA	40 (10)	70	59 ± 5	75 ± 30	163 ± 70	15 (7)		
Tg(HuAPP$_{695}$.WTmyc)6214	4 ± 0.3	<0.05	NA	0	>350			56 (36)		
Tg(HuAPP$_{695}$.WTmyc)466	26 ± 1.2	1.0 ± 0.21	0 (12)	0	>250			6 (0)	– (0/1)	–
Tg(HuAPP$_{695}$.WTmyc)6209	28 ± 6.1	1.6 ± 0.43	NA	19	115 ± 8	156 ± 47		78 (37)		
Tg(HuAPP$_{695}$.TRImyc)1072	4 ± 0.2	<0.05	NA	0	>350			52 (49)		
Tg(HuAPP$_{695}$.TRImyc)1056	7 ± 1.7	0.3 ± 0.09	0 (10)	0	>350			40 (36)		
Tg(HuAPP$_{695}$.TRImyc)1118	21 ± 3.7	1.4 ± 0.17	19 (48)	33	93 ± 10			64 (43)	+ (1/1)	–
Tg(HuAPP$_{695}$.TRImyc)1140	49 ± 2.5	2.0 ± 0.32	54 (35)	27	74 ± 7	103 ± 1	112 ± 7	58 (35)		
Tg(HuAPP$_{695}$.TRImyc)1130H	74 ± 3.7	3.6 ± 0.54	84 (68)	60	70 ± 2	87 ± 4	110 ± 8	114 (27)	+ (3/3)	–
Tg(MoAPP$_{695}$.WT)1859	6 ± 0.8	0.8 ± 0.09	0 (14)	0	>350			14 (0)		
Tg(MoAPP$_{695}$.WT)1855	24 ± 1.3	2.7 ± 0.1	37 (19)	0	169 ± 27			27 (24)		
Tg(MoAPP$_{695}$.WT)1874	31 ± 3.7	3.1 ± 0.55	54 (54)	11	72 ± 3	119 ± 6		27 (13)	+ (3/5)	
Non-Tg mice	0	0	0 (100)	0	>500			164 (135)	+ (6/7)	
Founders or first generation only[i]										
Tg(HuAPP$_{695}$.TRImyc)1057F	64–128[h,i]	NA	100 (1)	100					+ (1/1)	–
Tg(HuAPP$_{695}$.TRImyc)1138	64–128[h,i]	NA	75 (4)	100					+ (2/2)	–
Tg(HuAPP$_{695}$.SWE)1844F	42[h]	NA	NA (1)	100					+ (1/1)	–
Tg(HuAPP$_{695}$.SWE)1837F	42[h]	NA	NA (1)	100					+ (1/1)	–
Tg(HuAPP$_{695}$.SWE)1827F	59[h]	NA	NA (1)	100					+ (1/1)	–
Tg(HuAPP$_{695}$.SWE)1665F	244[h]	NA	100 (1)	NA					+ (1/1)	–
Tg(MoAPP$_{695}$.WT)1869	26[h]	NA	75 (4)	67					+ (1/2)	

[a] H indicates high copy transgene array in founders harboring two or more transgene arrays. F indicates only the founder was studied, owing to poor breeding.
[b] Determined for ≥3 animals per line unless indicated.
[c] Relative to endogenous MoAPP = 1, determined for ≥3 animals per line.
[d] Defined by corner index test.
[e] Excluding animals sacrificed for other studies. Because not all "dead" animals exhibit neophobia prior to death, the percentage dead may be greater than the percentage sick.
[f] Number in parentheses indicates number of animals that did not die naturally. This number includes animals removed form the study to provide material for pathological or laboratory study.
[g] Detectable using 6E10 antibody.
[h] Determined for a single animal.
[i] Determined by serial dilution.
[j] These animals developed behavioral abnormalities and died early, preventing the establishment of stably breeding lines.

breeding beyond the first generation in founders and lines harboring >74 copies of $HuAPP_{695}$.TRImyc and in 1 line of mice harboring 26 copies of $MoAPP_{695}$.WT. These observations indicate that overexpression of Tg APP beyond a critical level is highly deleterious, precluding the establishment of permanent lines (Table 2).

Death rates depended directly upon levels of APP expression (Table 2; see Figure 4a). To assess the relative effects of transgenes with distinct genotypes, we determined the incidence of death during the first 100 days of life in lines expressing different levels of HuAPP or MoAPP. Death rates were higher in Tg mice expressing mutant and wild-type HuAPP than in Tg mice expressing comparable levels of wild-type MoAPP. Comparisons of Tg mice expressing mutant versus wild-type HuAPP were not possible over the full range of APP expression. In most lines (e.g., Tg6209 and Tg1118), a fraction of animals survived long term (>250 days). The longevity of these survivors extended beyond that predicted by survival curves derived from other mice in the same line (Figure 3).

In <10% of animals, death followed a period of several days during which the mice were ungroomed, kyphotic, hypothermic, cachexic, and unresponsive when touched or gently prodded. About 14% of Tg($HuAPP_{695}$.TRImyc) mice overexpressing APP exhibited agitation, thigmotaxis, or inactivity without neophobia (defined by the corner index test described below) and died as early as 1 month of age. A few mice died immediately after a witnessed tonic-clonic seizure. The majority of Tg($HuAPP_{695}$.TRImyc) and Tg(MoAPP.WT) animals overexpressing APP died after they were formally diagnosed by corner index criteria but prior to appearing moribund. These mice probably died suddenly, since most were found dead within 2–16 hr of having been examined for neophobia, where they performed poorly but were not obviously moribund. Gross and microscopic examinations of 6 Tg($HuAPP_{695}$.TRImyc) mice found dead revealed normal appearance, size, and regional development of the brain, with characteristic gliotic brain pathology (described below) but no amyloid or evidence of microscopic or gross pathology outside the CNS. The cause of sudden death in these mice is unknown but may be related to seizures or neurogenic arrythmias.

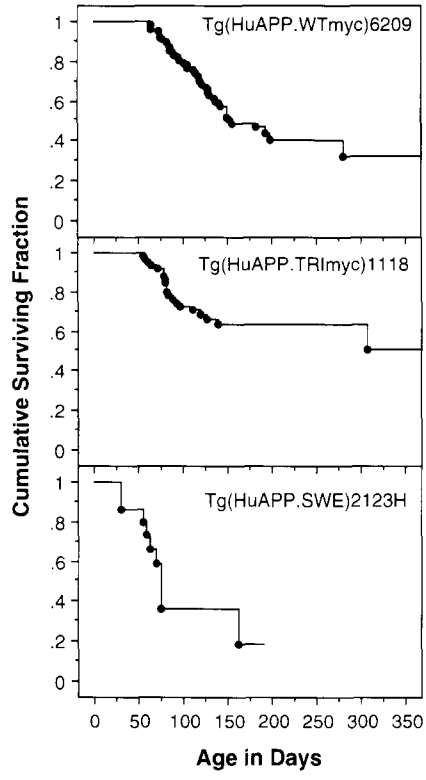

Figure 3. Survival in 3 Lines of FVB/N Mice Overexpressing APP

Kaplan–Meier survival curves for Tg($HuAPP_{695}$.WTmyc)6209 (top), Tg($HuAPP_{695}$.TRImyc)1118 (middle), and Tg($HuAPP_{695}$.SWE)2123H (bottom) are shown. Calculations include animals that were removed from the study for analysis in addition to long-term survivors. The curves illustrate the occurence of long-term survivors among Tg lines overexpressing APP in spite of early death in a proportion of each line. For Tg($HuAPP_{695}$.WTmyc)6209, 3 mice survived over 350 days, with the oldest (2) currently 605 days old. The oldest surviving mice from the Tg($HuAPP_{695}$.TRImyc)1118 and Tg($HuAPP_{695}$.SWE)2123H lines are 375 and 191 days of age. Results to date suggest that the risk of death for Tg mice surviving longer than 200 days does not differ significantly from that for non-Tg mice.

Behavioral Abnormalities

Neophobia and Other Neurologic Signs

In some Tg mice, we noticed an unusual behavior characterized by transient cessation in exploratory activity specific to testing in a novel chamber. To study this behavior quantitatively, we devised a simple behavioral test, the corner index test, that revealed a striking difference between Tg and non-Tg mice. Corner index scores for non-Tg mice showed few values ≤ 1 during the first 3 months, while scores of some Tg mice overexpressing APP showed values ≤ 1 with advancing age. The low scores appear to reflect a neophobic response because no differences in locomotor activity or exploratory motivation between non-Tg and Tg mice were detectable in Y maze performance (described below). Based on >2000 tests of >100 Tg mice and >2500 tests of >140 non-Tg mice <150 days of age, the age when two scores of "0" or a "0" and "1" appeared within three consecutive testing sessions defined the onset of neophobia. None of the 100 non-Tg mice tested through 100 days of age or of the 48 non-Tg mice tested through 150 days of age failed the corner index test. Neophobia developed as early as 1 month of age in both male and female Tg mice overexpressing APP and preceded death by an average of 40 days in Tg1130H mice. Six Tg FVB/N lines and 4 additional founders expressing high levels of wild-type $MoAPP_{695}$.WT, $HuAPP_{695}$.SWE, $HuAPP_{695}$.WTmyc, or $HuAPP_{695}$.TRImyc exhibited neophobia (see Table 2). Mice failing the corner index test also exhibited other neurologic signs, including thigmotaxis, agitation, stiff tail, stare, tremulousness, and inactivity. Of 181 mice from affected lines, 6 had generalized tonic-clonic seizures during corner index testing. To ensure that neophobia and early death were not artifacts of overexpression of a foreign (human) species of protein and to determine whether these abnormalities could be

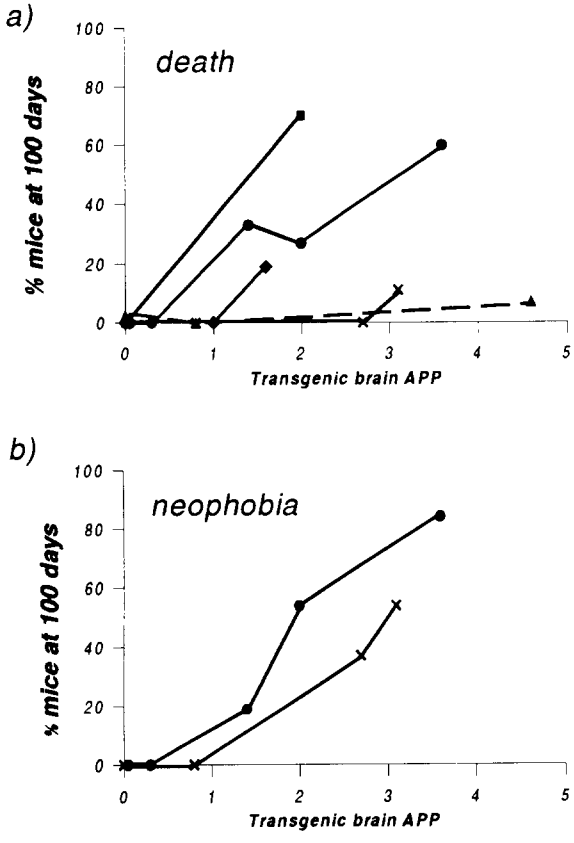

Figure 4. Dependence of Death and Neophobia upon Transgenic Brain APP Expression, APP Genotype, and Host Strain

(a) Death rates during the first 100 days of life were determined for Tg FVB/N mice (solid lines) expressing different levels of $HuAPP_{695}$.SWE (squares), $HuAPP_{695}$.TRImyc (circles), $HuAPP_{695}$.WTmyc (diamonds), and wild-type MoAPP (crosses) and for Tg C57B6 × (C57B6/SJL)F1 mice (dashed line) expressing $HuAPP_{695}$.SWE (triangles). For levels of APP expression >1, a larger fraction of mice died expressing $HuAPP_{695}$.TRImyc, $HuAPP_{695}$.SWE, or $HuAPP_{695}$.WTmyc than wild-type MoAPP, indicating that death rates are greater for mutant and wild-type HuAPP than for wild-type MoAPP, and that APP overexpression per se is not the cause of death. Tg($HuAPP_{695}$.SWE)C57B6 × (C57B6/SJL)F1 mice exhibited significantly lower rates of mortality than Tg FVB/N mice expressing either $HuAPP_{695}$.TRImyc or $HuAPP_{695}$.SWE, demonstrating a pronounced effect of host strain on mortality. The Tg APP level in Tg FVB/N mice expressing $HuAPP_{695}$.SWE was interpolated using information shown in Figure 2 and known Tg copy numbers; too few mice were generated, owing to poor breeding behavior and early death, to enable direct APP analyses.

(b) The development of neophobia during the first 100 days was determined for Tg FVB/N mice expressing different levels of $HuAPP_{695}$.TRImyc (circles) and wild-type MoAPP (crosses). For levels of APP expression >1, the occurrence of neophobia is higher for Tg mice expressing $HuAPP_{695}$.TRImyc.

accelerated by endogenous MoAPP, we generated Tg FVB/N mice overexpressing wild-type MoAPP; 37% of Tg1855 and 54% Tg1874 mice were neophobic at 100 days, and 11% of Tg1874 mice were dead at 100 days (see Table 2). The rate of development of neophobia was lower in Tg mice expressing $MoAPP_{695}$.WT than in Tg mice expressing $HuAPP_{695}$.TRImyc, paralleling the lower death rates in Tg($MoAPP_{695}$.WT) mice (Figure 4b).

To determine whether non-Tg FVB/N mice, with an average lifespan of 2 years, become behaviorally impaired with advancing age, 110 FVB/N mice 150–500 days of age from three different institutions (University of Minnesota, Minneapolis, Minnesota; McLaughlin Research Institute, Great Falls, Montana; Harlan Sprague Dawley, Inc., Indianapolis, Indiana) were studied for behavioral abnormalities. With advancing age, 15 mice of both sexes developed neophobia (defined by the corner index test) along with agitation and inactivity as early as 154 days of age, 3 had seizures, several died prematurely (excluding mice sacrificed for studies), and 6 mice died from tumors or accidentally. One death occurred immediately following a seizure; the other mice died suddenly of unknown causes. Several neophobic mice grew progressively less active and were sacrificed between 9 and 91 days after the onset of the disorder. The cumulative incidence of neophobia in this cohort of FVB/N mice was ~20% by 500 days of age.

Impaired Spatial Alternation in Tg FVB/N Mice

Tg FVB/N mice were assessed for spontaneous alternation behavior in a Y maze, a task thought to involve the hippocampus (Douglas, 1990). Neophobia in Tg mice expressing either $MoAPP_{695}$.WT or $HuAPP_{695}$.TRImyc was associated with diminished spontaneous alternation (Figures 5b and 5e). (Mice overcame neophobia in the Y maze during the initial 5 min free exploration interval.) There was no significant difference in the number of maze arm entries made by 24 neophobic Tg (39.9 ± 6.44, mean ± SEM) and 24 age-matched non-Tg (45.8 ± 5.61) mice, indicating that potential differences in locomotor activity and exploratory motivation cannot explain the different rates of spontaneous alternation. Impaired spontaneous alternation was observed in Tg($HuAPP_{695}$.TRImyc) mice not yet neophobic by corner index criteria but already showing signs of slowness and thigmotaxis (Figure 5d), indicating that impaired spatial alternation precedes neophobia. No significant difference was observed between 9-week-old Tg($MoAPP_{695}$.WT) mice showing signs of inactivity and thigmotaxis, but not yet neophobic by corner index criteria, and non-Tg littermates (Figure 5a); however, the relatively low scores obtained by both experimental and control subjects in this experiment may have obscured a difference. Five-week-old Tg($HuAPP_{695}$.TRImyc) mice exhibiting no clinical abnormalities showed no impairment of spatial alternation compared with non-Tg littermates (Figure 5c), obtaining significantly higher scores than 8- or 11-week-old Tg mice ($p = .0432$, t test), indicating that abnormal spatial alternation in Tg FVB/N mice overexpressing APP is an acquired trait.

Regional Cerebral Glucose Utilization

To identify the affected areas of the brain in neophobic Tg and neophobic mid- to late-adult non-Tg FVB/N mice, regional brain glucose utilization was determined by densitometric measures of [^{14}C]deoxyglucose levels (μCi/100 g/min). Regional cerebral glucose utilization in neophobic Tg1130H and age-matched non-Tg mice was compared. The former possess significant reductions in glucose utili-

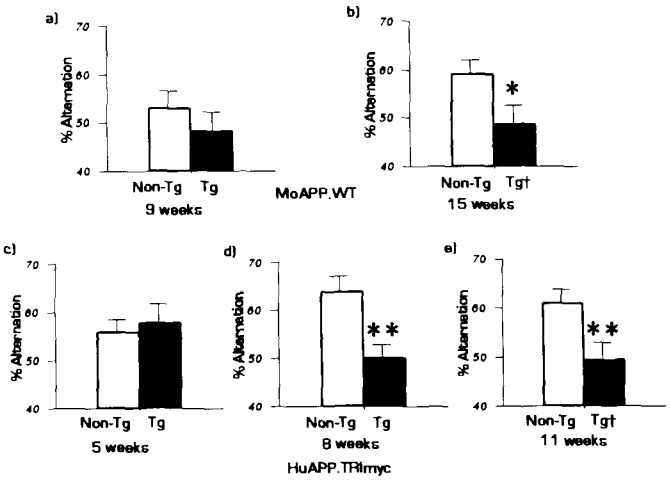

Figure 5. Impaired Spontaneous Alternation in a Y Maze

The values shown represent the percentage alternation during an 8 min period (mean ± SEM). The following groups were tested: (a) 11 Tg(MoAPP$_{695}$.WT)1874 transgene-positive mice showing signs of inactivity but not yet meeting criteria for neophobia and 11 transgene-negative littermates (9 weeks old); (b) 11 Tg(MoAPP$_{695}$.WT)1874 transgene-positive neophobic mice (dagger) and 12 transgene-negative littermates (15 weeks old); (c) 6 Tg(HuAPP$_{695}$.TRImyc)1130H and 4 Tg(HuAPP$_{695}$.TRImyc)1140 transgene-positive mice showing no abnormal neurologic signs and 15 transgene-negative littermates (5 weeks old); (d) 12 Tg(HuAPP$_{695}$.TRImyc)1130H transgene-positive mice showing signs of inactivity but not yet meeting criteria for neophobia and 12 transgene-negative littermates (8 weeks old); and (e) 5 Tg(HuAPP$_{695}$.TRImyc)1130H and 7 Tg(HuAPP$_{695}$.TRImyc)1140 transgene-positive neophobic mice (dagger) and 12 transgene-negative littermates (11 weeks old). Two Tg(MoAPP$_{695}$.WT)1874 transgene-positive mice were excluded because they made too few entries (<12) to determine an accurate alternation score. Differences between transgenic and nontransgenic mice were compared using a two-tailed Student's t test (single asterisk, $p < .05$; double asterisk, $p < .01$).

zation in various cortico-limbic regions, including the entorhinal cortex (−37%; p = .008), hippocampus (−30%; p ≤ .003), and amygdala (−28%; p = .004) as well as the parietal (−34%; p = .001), temporal (−33%; p = .017), and occipital (−36%; p = .001) lobes of the cerebral cortex (Table 3; Figure 6). The somatosensory-motor cortex was relatively spared, corroborating the apparent absence of motor and sensory abnormalities in these mice, and many brain stem regions, including the pontine reticular formation, vestibular nuclear complex, and dentate nucleus, showed no significant reduction in glucose utilization.

Comparisons of regional brain glucose utilization in neophobic mid- to late-adult non-Tg FVB/N mice compared with behaviorally normal, age-matched FVB/N mice revealed significant decreases in regional glucose utilization in several areas of the cerebrum, particularly the entorhinal cortex (−45%; p < .001), hippocampus (−33%; p < .001), amygdala (−30%; p = .003), hypothalamus (−34%; p = .004), and caudate-putamen (−14%, p < .001), as well as the parietal (−16%; p = .027) and temporal (−17%; p = .019) lobes of the cerebral cortex. In contrast, no significant decreases were observed in brainstem structures (p > .05), with the exception of the inferior colliculus (−22%; p = .015). The somatosensory-motor cortex was notably less affected, as in neophobic Tg FVB/N mice. The pattern of regional brain glucose utilization in Tg mice overlapped strikingly with that of aged, impaired non-Tg mice. With the sole exception of the inferior colliculus, every affected area in aged, impaired non-Tg mice was also significantly reduced in the younger Tg mice.

Astrogliosis without Amyloid Formation in Brains of Transgenic FVB/N Mice

Using coded specimens, we examined brains of 19 neophobic Tg mice expressing HuAPP$_{695}$.SWE, HuAPP$_{695}$.WTmyc, HuAPP$_{695}$.TRImyc, or MoAPP$_{695}$.WT as well as 12 age-matched, unaffected non-Tg mice (see Table 2). Fifteen brains from affected Tg mice exhibited prominent hypertrophic astrocytes located predominantly in the parahippocampal area, hippocampus, amygdala, and cerebral cortex (Figure 7a), with relative sparing of the basal ganglia. The astrocytes had enlarged, elongated processes when immunostained for glial fibrillary acidic protein (GFAP), and there was no apparent increase in the number of astrocytes. Brains of age-matched non-Tg mice were devoid of reactive gliosis. In general, there was an association between gliosis and abnormal behavior (Yates-corrected χ^2 = 14.83, p = .00012). Bielschowsky silver stains revealed no neurofibrillary tangles, dystrophic neurites, or neuritic plaques. Neurons appeared normal with Nissl and hematoxylin and eosin stains.

Seven non-Tg FVB/N mice 9–12 months of age exhibiting neophobia and 9 age-matched, behaviorally normal mice were examined in a coded fashion. Six of the 7 brains from neophobic mice exhibited pronounced astrocytic gliosis in the hippocampus, parahippocampal area, amygdala, and cerebral cortex as detected by GFAP staining (Figure 7c). The neostriatum showed little or no astrocytosis. None of the brains from the 9 age-matched, behaviorally normal mice exhibited this degree of gliosis, although modest gliosis restricted to the hippocampus was observed in some control FVB/N mice. These findings indicate that neophobia in non-Tg FVB/N mice is associated with gliosis in the cerebral cortex and limbic brain regions (Yates-corrected χ^2 = 8.96, p = .003). The brains of these mice showed no amyloid deposition, neurofibrillary tangles, neuronal abnormalities, or qualitative changes in neuronal or glial numbers. To detect APP or Aβ immunoreactivity in brain tissue from animals with clinical abnormalities in Tg FVB/N lines overexpressing HuAPP, we used two antibodies: 8E5 antibody, which stained amyloid and intraneuronal vesicular structures in microwaved tissue

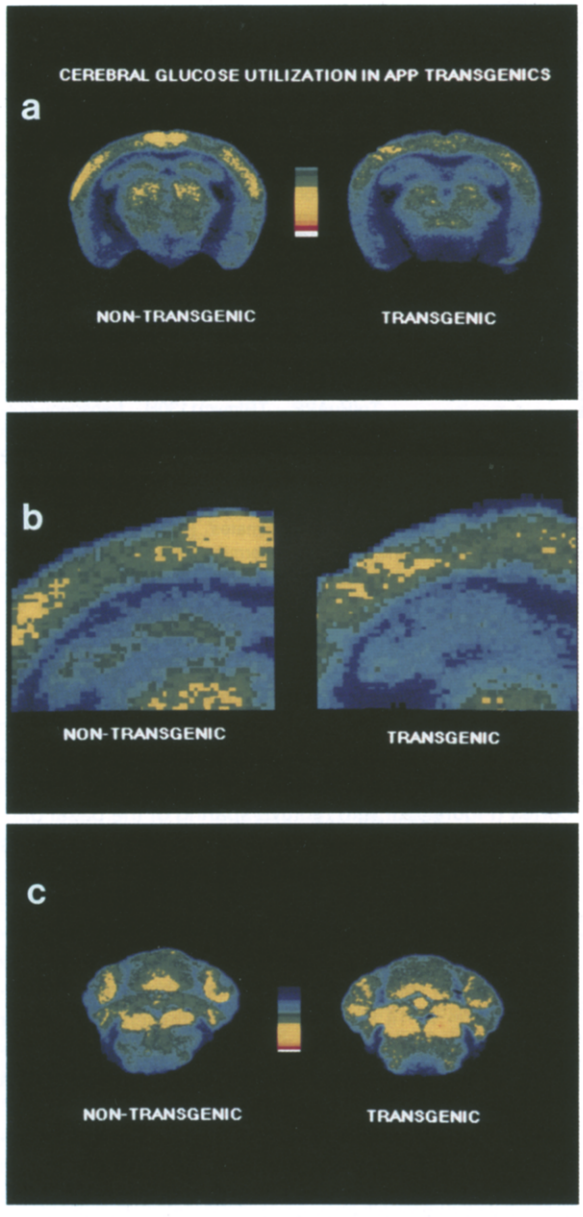

Figure 6. Regional Brain Glucose Hypo-Utilization in Transgenic Mice

(a) Coronal sections through cerebral cortex, hippocampus, and anterior brainstem of a neophobic Tg(HuAPP$_{695}$.TRImyc)1130H mouse and a non-Tg littermate. Optical density ratios were color coded. Blue and black represent lowest optical density ratios; red and white represent highest optical density ratios.

(b) Enlarged view of hippocampus and overlying cerebral cortex showing diminished glucose utilization in both regions in the Tg mouse.

(c) Coronal sections through cerebellum and posterior brainstem showing no diminution in glucose utilization in Tg mouse.

sections from patients with AD, and 6E10 antibody, which stains amyloid from patients with AD only after formic acid pretreatment of brain tissue. In 4 Tg(HuAPP$_{695}$.SWE) mice and 7 Tg(HuAPP$_{695}$.TRImyc) mice, neither the microwave nor formic acid pretreatment of brain tissue revealed extracellular APP or Aβ immunoreactivity using these antibodies. Amyloid deposits were not demonstrable by staining with Congo red or thioflavin S. We concluded that the abnormal phenotype in these Tg mice occurred independently of amyloid plaque deposition.

Host Strain Effect upon Mortality in Transgenic Mice Overexpressing APP

To assess effects of host strain upon mortality in Tg mice expressing HuAPP transgenes, animals were created in (C57B6/SJL)F1 embryos backcrossed to C57B6 breeders. We examined 28 Tg mice from Tg(HuAPP$_{695}$.SWE)C57-B6 × C57B6/SJL-2576 mice expressing HuAPP with the Swedish mutation at a level >4-fold over that of endogenous brain APP (higher than in any Tg FVB/N lines overexpressing APP). These mice bred well and showed no difference in death rates when compared with 39 non-Tg littermates (see Figure 4a). Three Tg and 2 non-Tg mice died within the first 4 months of unknown causes. Ten Tg2576 mice appear well at 8 months of age, having outlived all 13 Tg FVB/N mice from 4 founders harboring ~40 copies of the HuAPP$_{695}$.SWE transgene with an estimated 2-fold overexpression of Tg APP.

Discussion

FVB/N mice overexpressing mutant and wild-type APP transgenes die early and possess clinical abnormalities, including impaired spatial alternation, neophobia, agitation, inactivity, seizures, diminished regional brain glucose utilization, and hypertrophic astrogliosis in the cerebrum without amyloid plaques. We have identified three parameters that influence the development of clinical abnormalities in Tg mice expressing APP: levels of APP expression, primary structure of APP transgenes, and host strain. C57B6 × (C57B6/SJL)F1 hybrid mice overexpressing mutant HuAPP live significantly longer than FVB/N mice expressing the same Tg APP, demonstrating a host strain effect upon the resultant phenotype. The clinical abnormalties in Tg FVB/N mice closely resemble those occurring in a subset of older non-Tg FVB/N mice, suggesting that overexpression of APP accelerates a naturally occurring, age-related CNS disorder in this strain of mice.

Transgenic APP Expression

Until overexpression of APP and APP fragments was achieved, there were no reports of robust clinical or pathological phenotypes in multiple lines of Tg mice (Sandhu et al., 1991; Yamaguchi et al., 1991; Kammesheidt et al., 1992; Buxbaum et al., 1993; Lamb et al., 1993; Pearson and Choi, 1993). Some transgenic mice have been reported with rare Aβ deposits and age-related memory deficits (Quon et al., 1991; Higgins et al., 1994; Moran et al., 1995). Neuronal apoptosis associated with seizures and death was observed in Tg FVB/N mice overexpressing cytoplasmic Aβ (LaFerla et al., 1995), and abundant cerebral amyloid deposition was reported in Tg mice expressing mutant HuAPP exceeding endogenous levels by 5–10 times (by qualitative Western blot; Games et al., 1995). Tg APP expression in our mice with the highest APP levels was comparable to that in mice described by Games et

Table 3. Regional Brain Glucose Utilization Index in Healthy versus Neophobic Aged FVB/N Mice and in Healthy Nontransgenic versus Neophobic FVB/N Mice

Brain Regions	Aged Healthy (mean ± SEM)	Aged Neophobic (mean ± SEM)	t Test (p)	Non-Tg Healthy (mean ± SEM)	Tg1130H Neophobic (mean ± SEM)	t Test (p)
CxE[a]	1.32 ± 0.12	0.73 ± 0.08	<.001	1.08 ± 0.09	0.68 ± 0.06	.008
HpA[a]	1.13 ± 0.06	0.76 ± 0.04	<.001	1.05 ± 0.06	0.73 ± 0.06	.003
HpP[a]	1.05 ± 0.03	0.86 ± 0.01	<.001	1.10 ± 0.06	0.79 ± 0.05	.002
CP[a]	1.32 ± 0.03	1.13 ± 0.03	<.001	1.33 ± 0.08	1.09 ± 0.05	.048
Amg[a]	0.79 ± 0.05	0.55 ± 0.05	.003	0.74 ± 0.04	0.53 ± 0.05	.004
Ht[a]	0.71 ± 0.07	0.47 ± 0.05	.004	0.74 ± 0.04	0.58 ± 0.04	.015
IC	1.38 ± 0.13	1.07 ± 0.02	.015	1.61 ± 0.06	1.58 ± 0.12	NS
CxT[a]	1.09 ± 0.08	0.90 ± 0.05	.019	1.10 ± 0.08	0.74 ± 0.11	.017
CxP[a]	1.52 ± 0.06	1.27 ± 0.11	.027	1.34 ± 0.07	0.88 ± 0.08	.001
SC	1.31 ± 0.06	1.18 ± 0.07	NS	1.26 ± 0.06	0.94 ± 0.07	.003
GP	0.80 ± 0.08	0.68 ± 0.03	NS	0.96 ± 0.09	0.61 ± 0.06	.013
TV	1.49 ± 0.09	1.30 ± 0.18	NS	1.24 ± 0.06	0.83 ± 0.08	.002
HM	0.96 ± 0.05	1.01 ± 0.04	NS	1.05 ± 0.05	0.97 ± 0.01	NS
CxO	1.31 ± 0.09	1.21 ± 0.08	NS	1.23 ± 0.05	0.79 ± 0.09	.001
PRF	0.87 ± 0.08	0.84 ± 0.08	NS	0.97 ± 0.04	0.91 ± 0.04	NS
cc	0.59 ± 0.07	0.51 ± 0.06	NS	0.84 ± 0.06	0.71 ± 0.08	NS
CxF	1.37 ± 0.06	1.28 ± 0.12	NS	1.37 ± 0.08	1.14 ± 0.08	NS
VC	1.50 ± 0.08	1.58 ± 0.22	NS	1.52 ± 0.07	1.45 ± 0.06	NS
TA	1.61 ± 0.07	1.51 ± 0.17	NS	1.42 ± 0.10	1.03 ± 0.07	.010
TR	1.45 ± 0.09	1.39 ± 0.13	NS	1.37 ± 0.06	0.95 ± 0.09	.002
CxSM	1.53 ± 0.06	1.46 ± 0.19	NS	1.36 ± 0.11	1.15 ± 0.07	NS
SN	0.92 ± 0.03	0.91 ± 0.03	NS	0.99 ± 0.06	0.76 ± 0.06	.018
DN	1.11 ± 0.09	1.12 ± 0.12	NS	1.20 ± 0.05	1.17 ± 0.04	NS
VM	1.07 ± 0.05	1.11 ± 0.01	NS	1.24 ± 0.04	1.14 ± 0.03	NS

Neophobic animals were identified by the corner index test. For each animal, glucose utilization within every brain region was normalized to the whole cerebellar value, since the cerebellum was devoid of clinical and pathological abnormalities. Statistical analyses between age-matched aged mice and age-matched non-Tg and Tg mice were performed using an unpaired Student's t test (NS, not significant, $p > .05$). Average ages for aged healthy, aged neophobic, non-Tg healthy, and Tg1130H neophobic mice were 429.3 ± 39.3 (n = 4), 429.3 ± 39.3 (n = 4), 98.1 ± 13.9 (n = 8), and 84.5 ± 4.74 (n = 6), respectively.

[a] Brain regions with significantly diminished glucose utilization indices in both aged and Tg impaired mice.

CxE, entorhinal cortex (also called parahippocampal area); HpA, anterior hippocamput (containing CA1–3 fields); HpP, posterior hippocampus; CP, caudate-putamen (also called striatum); Amg, amygdala; Ht, hypothalamus; IC, inferior colliculus; CxT, temporal cortex; CxP, parietal cortex; SC, superior colliculus; GP, globus pallidus; TV, ventral thalamic nucleus; HM, cerebellar hemisphere; CxO, occipital cortex; PRF, pontine reticular formation; cc, corpus callosum; CxF, frontal cortex; VC, vestibular nuclear complex; TA, anterior thalamic nucleus; TR, thalamic reticular nucleus; CxSM, somatosensory-motor cortex; SN, substantia nigra; DN, dentate nucleus; VM, cerebellar vermis.

al. All our Tg FVB/N lines expressing supra-endogenous levels of Tg APP developed clinical abnormalities within the first 100 days of life.

Three observations argue against the abnormal phenotype in our Tg mice being due to a nonspecific effect of Tg protein overexpression. First, the onset of neophobia and the age at death were influenced by specific transgene genotypes: mutant HuAPP conferred the disorder with higher age-related penetrance than wild-type MoAPP for similar levels of expression. Second, the total burden of brain APP in some affected Tg lines was only twice endogenous levels. *Even in animals that expressed >4 times the normal level of APP, the unchanged levels of brain PrP, which like APP undergoes processing through the secretory pathway, argues against a nonspecific effect of mere protein overexpression taxing the cellular machinery* for mRNA processing, protein sythesis, or protein modification. Third, Tg FVB/N mice harboring hamster PrP cosmid transgenes overexpressing PrP with a mutation linked to Gerstmann–Sträussler–Scheinker disease (GSS), a dominantly inherited neurodegenerative disorder, develop an entirely distinct phenotype with ataxia and spongiform degeneration (T. Haga and S. Prusiner, personal communication).

The absence of changes in endogenous mouse PrP levels between Tg and non-Tg mice also makes it unlikely that an artifact of supernumerary transgenes resulted in competitive inhibition of PrP transcription factors. In addition, a previously published line of Tg FVB/N mice expressing human PrP driven by equivalently high or higher transgene copies of the hamster PrP gene cosmid vector exhibited none of the behavioral or pathological abnormalities observed in Tg APP mice (Telling et al., 1994), *weighing against nonspecific effects of the 5′ or 3′ untranslated regions in the PrP cosmid vector or other PrP gene components.*

Primary Structure of APP

The distinction between age-dependent penetrance of death and neophobia for FVB/N mice expressing MoAPP and HuAPP transgenes indicates that APP transgenes with different amino acid sequences differ in their age-dependent potency as regards the effect. However, the qualitative features of the phenotype we observe in all Tg

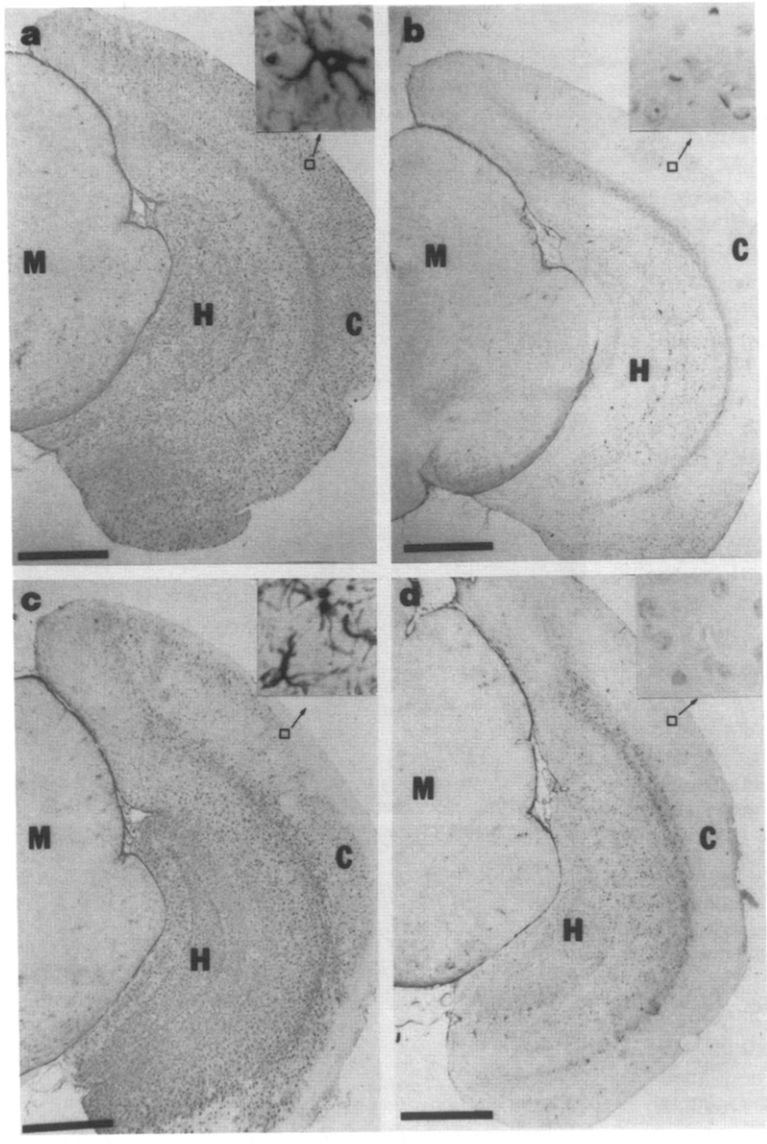

Figure 7. Cortico-Limbic Hypertrophic Astrocytic Gliosis in Transgenic and Nontransgenic FVB/N Mice Exhibiting Neophobia and Inactivity

Coronal sections of cortico-limbic and brainstem structures reacted with antibody to GFAP show hypertrophic gliosis in cortico-limbic areas of animals exhibiting behavioral abnormalities. C, cerebral cortex; H, hippocampus; M, midbrain.

(a) Tg(HuAPP$_{695}$.TRImyc)1118–334 exhibiting behavioral abnormalities (agitation and neophobia) at 144 days of age, sacrificed at 206 days.

(b) Non-Tg littermate of Tg(HuAPP$_{695}$.TRImyc) 1118–334 without behavioral abnormalities, age 206 days.

(c) Non-Tg #4565 exhibiting behavioral abnormalities (inactivity and neophobia) at 324 days of age, sacrificed at 334 days.

(d) Non-Tg littermate of #4565 without behavioral abnormalities, age 334 days.

FVB/N mice overexpressing APP resemble an acceleration of a naturally occurring CNS disorder in FVB/N mice, regardless of the primary structure of APP. Although it is possible that the presence of two additional transmembrane mutations in HuAPP.TRImyc could diminish generation of Aβ, and thereby alter the phenotype, our data indicate that mice expressing this transgene are in fact able to generate both Aβ$_{1-40}$ and Aβ$_{1-42}$ and develop the same clinical abnormalities as Tg mice expressing HuAPP$_{695}$.SWE, HuAPP$_{695}$.WTmyc, and MoAPP$_{695}$.WT transgenes. Given this consistent pattern of data, it is likely that FVB/N mice overexpressing other APP transgenes, including HuAPP.V717I lacking the extra mutations, would also exhibit a phenotype resembling the naturally occurring CNS disorder described here in FVB/N mice. This hypothesis is being tested.

Host Effects

There are two important reasons to express APP and APP mutants in Tg mice: first, to model AD, and second, to study the biologic activity of APP overexpression in vivo. Such studies must consider the influence of the host on the Tg phenotype because numerous genetic and biologic differences exist between humans and mice. For example, host modification of a pathological phenotype occurred in GSS modeled in Tg mice. Overexpression of a mutant PrP genetically linked to GSS produced spongiform neurodegeneration indistinguishable from murine scrapie, but the amyloid plaques that define GSS in humans occurred too infrequently to be seen in the majority of Tg mice (Hsiao et al., 1990, 1994; Prusiner and Hsiao, 1994). Another example of host modification has been described in FVB/N and (C57B6 × 129Sv)F1 mice harboring a disrupted keratin gene. When the disrupted keratin locus resides in (C57B6 × 129Sv)F1 mice, death during embryogenesis is observed, but in FVB/N mice, a mild skin disorder is observed (Baribault et al., 1994). We show here a third example of host modification of Tg phenotypes in FVB/N and C57B6 × (C57B6/SJL)F1 mice expressing the same mutant human APP transgene. When high levels of Hu-

Table 4. Transgenic Mice Overexpressing APP or Aβ

	This Paper	Games et al., 1995	LaFerla et al., 1995	Quon et al., 1991[a]
Transgenic proteins	Human APP Mouse APP	Human APP	Mouse Aβ–cytoplasmic (Mouse Aβ–secreted)[b]	Human APP
Transgene genotype	Wild type, K670N, M671L V7171, V721A, M722V	V717F	Wild type	Wild type
Promoters	PrP	PDGF	NF-L	NSE
APP isoforms	695	695, 751, 770	NA	751 (695)[c]
Highest brain expression	Cerebrum Cerebellum	Cerebrum Cerebellum	Cerebrum	Not reported
Target cells	Neurons Less in astrocytes	Neurons	Neurons	Neurons
APP levels	Comparable to Games, 1995 (qualitative Western) >8× (ECL, densitometry) 4.6× (^{125}I-protein A, phosphorimaging)	~10× (qualitative Western)	NA	Not quantified
Transgenic Aβ	Present	Present	Present	Present by ICC[e]
Behavioral phenotype	Neophobia Impaired spatial alternation in Y maze Agitation, inactivity Seizures	None reported	Seizures	Impaired spatial alternation in Y maze Impaired spatial memory in water maze
Lifespan	Early death (>50% by 1 year)[d]	Not reported	Early death (>50% by 1 year)	No early death reported
Brain physiology	Decreased glucose utilization in forebrain (especially entorhinal cortex, hippocampus, amygdala)	Not reported	Not reported	Not reported
Pathology	Cortico-limbic gliosis	Cortico-limbic amyloid Neuritic changes	Cortico-limbic gliosis Apoptosis Extracellular Aβ deposits	Rare APP deposits Tau immunoreactivity
Mouse strain	FVB/N	Swiss Webster × (B6/D2)F1	FVB/N	JU

[a] See also Higgins et al., 1994, and Moran et al., 1995.
[b] No phenotypic abnormalities reported.
[c] No phenotypic abnormalities reported.
[d] Tg mice expressing supra-endogenous levels of HuAPP or MoAPP.
[e] Detected by immunocytochemical analysis.

APP with the Swedish mutation were expressed in FVB/N mice, >70% of mice died by 100 days of age; however, <10% of C57B6 × (C57B6/SJL)F1 mice expressing higher levels of the same transgene died during the same age interval. It is very common for mutations to be too deleterious to be maintained in standard inbred mouse strains. For instance, most inbred mice homozygous for the grey tremor mutation die by 3 months of age, but on outbred genetic backgrounds, many survive and reproduce (Kinney and Sidman, 1986). Therefore, it will be important both to distinguish the protean manifestations of Tg APP expression in different pure and hybrid strains of mice and to identify features occurring in common. It is possible that the specific features associated with Tg APP expression in FVB/N mice involve particular genes, which may be possible to identify through genetic analyses. The same approach may reveal the genes that are responsible for distinct phenotypes in various other inbred strains.

The existence of long-term survivors in some Tg FVB/N lines overexpressing APP implies that other, as yet unknown factors besides APP levels, APP primary structure, and host strain can influence the phenotypes of individual Tg mice. In these Tg lines, the sharp drop in mortality after ~150–200 days implies that vulnerable periods exist in an animal's life, during which at least some of the deleterious effects of APP overexpression are more likely to manifest. We are exploring the possibility that extracellular Aβ deposits are more likely to appear in long-term survivors since Aβ deposits have been found only in older Tg mice expressing APP (Higgins et al., 1994; Games et al., 1995).

Other Transgenic APP Paradigms

A summary of four Tg paradigms overexpressing APP or Aβ is presented in Table 4. There are two apparent discrepancies between the clinical, neuropathologic, and functional appearances of our Tg FVB/N mice expressing mutant APP transgenes and the Tg mice with amyloid deposits (Games et al., 1995); our mice displayed behavioral and functional abnormalities, but lacked amyloid deposits. Levels and regions of APP expression were comparable and cannot explain the different phenotypes. Whether the discrepant clinical and neuropathologic appearances of our FVB/N mice expressing high levels of APP and the hybrid mice of Games et al. are due to host

strain differences or transgene disparities is under investigation.

On the other hand, the similar clinical and pathological features in FVB/N mice overexpressing APP and cytoplasmic Aβ (LaFerla et al., 1995) support the importance of host influences upon Tg phenotypes. The differences between these Tg mice may be due to distinctions between APP and Aβ expression and the cellular processing of these proteins, and to the respective levels of Aβ achieved in different mice. It is possible that FVB/N mice develop a lethal CNS disorder without developing amyloid plaques because they are more sensitive to the neurotoxic effects of Aβ (or some other component of APP), causing them to die before Aβ forms fibrils and precipitates. FVB/N mice might also lack the extracellular substrate molecules or cells facilitating Aβ precipitation. Alternatively, FVB/N mice might efficiently clear extracellular Aβ, impeding its aggregation to form plaques.

It has been suggested that APP transgenes containing the KPI domain (APP751 and APP770) produce memory deficits, whereas transgenes without the KPI domain may not be effective in this regard (Moran et al., 1995). Tg mice described by Moran et al. expressing APP_{751} were impaired in spatial alternation in a Y maze. Our Tg mice expressing APP transgenes lacking the KPI domain also exhibit impaired spatial alternation in a Y maze, indicating that, at least in FVB/N mice, this behavioral deficit can be induced by APP transgenes lacking the KPI domain.

APP, Aging, and AD

The CNS disorder in our Tg mice is directly related to overexpression of APP. Although the pathogenesis of the disorder appears to be due to activities of APP other than its ability to form extracellular amyloid deposits, it is still possible that Aβ mediates the pathogenic effects, since Aβ levels are elevated in Tg mice that develop neophobia and die. Murine Aβ secretion is enhanced in transfected murine cells expressing MoAPP (Araki et al., 1994), providing a similar rationale for the development of the CNS disorder in Tg mice expressing high levels of MoAPP. Moreover, cytoplasmic murine Aβ is neurotoxic in vivo (LaFerla et al., 1995). It is possible that the naturally occurring senescent disorder in older FVB/N mice represents a phenotypic continuum related to endogenous MoAPP expression. It will be critical to understand how aberrant APP metabolism can cause neuronal dysfunction without forming extracellular, congophilic aggregates.

We have shown that Tg FVB/N mice overexpressing APP exhibit impaired spatial alternation in a Y maze. Poor performance in this task has been speculated to reflect diminished motivation to explore novelty, inattention, or failure to remember acquired information (Gerlai et al., 1994). Since the task is believed to involve the hippocampus (Douglas, 1990), the significantly reduced levels of hippocampal glucose utilization in affected Tg mice corroborate the behavioral observation. Some other traditional tests of spatial memory (e.g., Morris water maze; Morris, 1984) could not be used to test our mice because FVB/N mice have poor visual acuity (Taketo et al., 1991). We are continuing to study memory and learning behavior in these mice but do not know if it will be possible to devise other tests that will overcome this obstacle. We therefore elected to make a direct observation of brain function in these mice by studying the specific distribution of regional glucose hypo-utilization.

The pattern of regional brain glucose hypo-utilization in Tg mice overlapped strikingly with that of aged, impaired non-Tg mice. The differences that were observed, as in the occipital cortex, superior colliculus, substantia nigra, and thalamic nuclei, may reflect ectopic expression of Tg APP, trans-synaptic effects, or a more advanced stage of the disorder. Regions associated with learning, memory, and affective behavior, such as the association areas of the cerebral cortex, hippocampus, entorhinal cortex, and amygdala, are the regions most affected both in cognitively impaired, aged humans and patients with AD (de Leon et al., 1983; Kumar et al., 1991) and in impaired Tg FVB/N mice and aged, impaired non-Tg FVB/N mice. Notably, the greatest decrease in glucose utilization in both Tg mice and aged, impaired non-Tg mice was in the entorhinal cortex, which is among the earliest brain structures involved in AD (Braak and Braak, 1991). Furthermore, the somatosensory-motor cortex was relatively spared in both Tg mice and aged, impaired non-Tg mice, as it is in humans with AD. Yet both the parietal and temporal lobes were significantly involved, as they are also in AD. Because we found no brain atrophy or neuronal loss, it is likely that glucose hypo-utilization in our mice reflects reduced glucose transport or metabolism rather than a reduction in the absolute number of neurons. A similar situation has been proposed in mildly demented AD patients (Kumar et al., 1991) and in AD patients showing reduced levels of CNS-specific glucose transporters, independently of neuronal or synaptic loss (Simpson et al., 1994). The remarkably analogous regional deficits in glucose utilization exhibited by humans with AD and FVB/N mice with both age- and APP-related brain impairment suggest that the disorders in humans and mice share at least some pathogenic mechanisms.

Since APP overexpression accelerates an age-related CNS disorder in FVB/N mice, it is possible that aberrant APP expression in each species or strain would give rise to age-dependent CNS dysfunction characteristic for each type of animal. Senescence is associated with a variety of alterations in rodent brains (Finch, 1993). Amyloid deposits and neurofibrillary tangles have not been documented as naturally occurring age-associated processes in these species. Studies of aged, cognitively impaired rodents have shown gliosis (Landfield et al., 1977) and diminished regional brain glucose utilization in the cerebrum (Gage et al., 1984), indicating that age-related CNS dysfunction occurs in rodents without Aβ deposition. Certain features of the age- and APP-related disorder observed in FVB/N mice appear to be distinctive for this mouse strain. The consistency with which the same neurological phenotype was observed in older FVB/N mice and younger mice expressing mutant HuAPP or higher levels of wild-type MoAPP parallels the occurrence of AD in older

humans and younger individuals with mutant APP or higher levels of wild-type APP, as in Down's syndrome. Studies of the effect of aberrant APP expression on age-dependent CNS dysfunction in different genetic backgrounds, as well as other species, would confirm or refute this line of reasoning.

Our studies indicate that age-dependent vulnerability of brain regions critical to learning, memory, and affective behavior in FVB/N mice can be accentuated by APP. However, our mice lacked the classical histological features used by pathologists to diagnose AD in humans, amyloid plaques and neurofibrillary tangles, and yet they displayed behavioral, physiological, and neuropathological characteristics strikingly similar to those of a subset of aged non-Tg mice of the same strain.

These data lead to the conclusion that APP overexpression can accelerate or accentuate a senescent CNS disorder in FVB/N mice without amyloid deposition in the brain. We speculate that some forms of senescence in the brains of other species may share a common biological origin with AD in humans. The histopathology of AD, particularly amyloid plaques, may thus be a useful diagnostic criterion for AD in humans but may not completely explain the pathogenesis of the human disorder. We suggest that the phenotypes of Tg animals expressing APP and other AD-associated genes (e.g., S182 and STM2) may be more completely understood if they are evaluated in the context of naturally occurring, age-dependent CNS dysfunction in the host and, when so understood, may cast further light upon the ultimate molecular and cellular abnormalities of AD.

Experimental Procedures

Transgene Construction

The PrP–APP transgenes were generated by inserting SalI-flanked human or mouse APP ORFs into a hamster PrP cosmid vector described in detail previously (Scott et al., 1992). This vector is a ~40 kb fragment of genomic DNA containing the hamster PrP gene with ~20 kb of upstream sequences, in which the hamster PrP ORF is replaced by a unique SalI restriction site. The $HuAPP_{695}$.SWE, $HuAPP_{695}$.TRImyc, and $HuAPP_{595}$.TRImyc APP sequences were modified for strong translation initiation. The 5′ end of the APP coding sequence is preceded by a SalI site and a strong Kozak translation initiation sequence (5′-**GTCGAC**ACCATGCTGCCC...), and the 3′ end of the APP coding sequence is immediately followed by a SalI site (...AACTAG**CAGCTG**-3′; start and stop codons are underlined; site in boldface). These modifications and the APP mutations were made using standard cloning methods and polymerase chain reacation (PCR)–based, site-directed mutagenesis. The PrP–APP cosmids were digested with NotI, which releases the PrP–APP fusion gene from the pcos6EMBL vector. The PrP–APP fusion genes were isolated after size fractionation on an agarose gel and electroeluted. The PrP–APP fusion gene was further purified with organic solvents and precipitated in ammonium acetate and ethanol. The PrP–APP fusion genes were dissolved in 5 mM Tris–Cl (pH 7.4) or 10 mM Tris–Cl (pH 8.0) to a final concentration of 2–4 μg/ml prior to embryo injection.

Transgenic Mouse Generation and Screening

Transgenic lines were initiated by microinjection of single-cell mouse embryos as described (Hogan et al., 1986). Embryo donors and fertile studs were inbred FVB/N mice obtained from the National Cancer Institute (NIH). Post-weaning tail biopsy DNA was generated as described (Hanley and Merlie, 1991); 1 μl of unpurified DNA was used in a 25 μl PCR reaction. To detect PrP–APP fusion DNA, the PrP–APP fusion DNA was amplified using the PCR with a pair of oligomer primers, 1503: (5′-CTGACCACTCGACCAGGTTCTGGGT-3′) and 1502 (5′-GTGGATAACCCCTCCCCCAGCCTAGACCA-3′), located in the 3′ region of APP and the 3′ untranslated region of PrP, respectively. The 1503 primer recognizes a region that is homologous in mouse and human APP and could therefore be used to detect both PrP–MoAPP and PrP–HuAPP DNA. Using primers 1502 and 1501 (5′-AAGCGGCC-AAAGCCTGGAGGGTGGAACA-3′), a parallel PCR reaction amplifying a fragment of murine PrP was performed as a positive control.

Transgene copy number analysis was performed using 5 μg of denatured purified tail DNA baked onto nitrocellulose and hybridized to a radiolabeled 1.3 kb SalI–XhoI DNA fragment encoding a segment of the hamster PrP 3′ untranslated region located in the hamster PrP cosmid vector (Scott et al., 1992). After two high stringency washes, the relative intensities of signals from genomic DNAs of transgenic mice and hamsters were compared using a phosphorimager to obtain transgene copy numbers relative to diploid hamster genomic DNA.

Analysis of Transgene Expression

APP transgene products were examined in progeny of transgenic founders sacrificed at 1–4 months of age. Quantitative immunoblotting of extracts from brain homogenates was carried out in parallel with extracts prepared from age-matched nontransgenic littermates. Homogenates (20%, w/v) of brain tissues were prepared in TNE (50 mM Tris–Cl [pH 8.0], 150 mM NaCl, 5 mM EDTA with 2% phenylmethylsulfonyl fluoride) buffer using a hand-held polytron. Homogenates were diluted with an equal volume of TNE, 1% Nonidet P-40, 1% Deoxycholate, 0.4% SDS and sonciated in a bath sonicator until all viscosity was lost. Homogenates were then boiled for 10 min and centrifuged at 10,000 × g for 10 min. The supernatants were mixed with an equal volume of 2× sample buffer (Laemmli, 1970), boiled 2 min, and fractionated using a 6% SDS–polyacrylamide gel. Proteins were electrophoretically transferred to Immobilon membranes (Pierce) and incubated with monoclonal (22C11 and 6E10) anti-APP antibodies. Reactive monoclonal antibodies were visualized following incubation with secondary rabbit antibodies to mouse IgG before incubation with ^{125}I–protein A. Radioactivity was quantified on a phosphorimager (Molecular Dynamics, Inc.).

Analysis of Aβ in Brain Tissue

Approximately 0.2 g of tissue was dounce homogenized (4 strokes) in 1 ml of 70% glass-distilled formic acid. Homogenates were centrifuged at >100,000 × g for 1 hr. The formic acid extract (layered between an overlaying lipid layer and a small pellet) was removed, and a small aliquot was diluted 50 times in 1 M Tris (pH 8.0). This sample was then further diluted 2.4 times in Buffer EC (0.02 M sodium phosphate [pH 7.0], 0.2 mM EDTA, 0.4 M NaCl, 0.2% bovine serum albumin, 0.05% CHAPS, 0.4% Block-Ace, 0.05% sodium azide), and 100 μl of this was analyzed directly using either the Ban50/Ba27 or Ban50/Bc05 ELISA systems described previously (Suzuki et al., 1994; Gravina et al., 1995). Aβ values reported were obtained by comparing the absorbance obtained from duplicate samples to standard curves of either $Aβ_{1-40}$ (Ban50/Ba27) or $Aβ_{1-42}$ (Ban50/Bc05) obtained from Bachem. These values were corrected for dilution and initial wet weight of the tissue and are expressed as picomoles per gram of wet weight. All samples were coded with respect to the transgenic status of the animals.

Behavioral Analyses

Neophobia

To perform the corner index test, a test mouse held by the tail is placed in the center of a cage (18 × 30 × 13 cm) with clean bedding (soiled bedding removed between tests), and the number of times the mouse sniffs the corners of the test cage during the first 30 s after being placed into the cage is recorded as the corner index (CI). Animals are usually tested 3 times per week. Low scores in animals housed alone were excluded from the analysis unless they displayed thigmotaxis or the characteristic freezing posture of other neophobic Tg mice. To control for variations in diurnal activity, all animals were tested between 1300 hr and 1830 hr. Criteria for the presence of neophobia in non-Tg mice >150 days of age was ≥3 consecutive scores of 0.

Spontaneous Alternation in a Y Maze

The apparatus was a symmetrical Y maze. Each arm measured 8 × 40 cm with 15 cm high side walls. The floor of the maze was open to allow a change of paper between each subject. Mice were placed in the center of the maze and allowed to explore freely for 5 min. Arms were arbitrarily designated A, B, and C, and the sequence of arm entries made in an 8 min period was used to measure alternation behavior: percentage alternation is the number of triads containing entries into all three arms (all three letters) divided by the total number of alternation opportunities (total number of arms entered − 2). Mice were coded and tested in random order.

Pathological Analyses of Mice

Brains of mice exhibiting behavioral abnormalities or found dead and age-matched littermates were examined for neuropathologic abnormalities. Brains were immersion fixed or perfused with 10% phosphate-buffered formalin or 4% buffered paraformaldehyde, embedded in paraffin, and cut into 5–8 μm sections. Tissue sections were stained with hematoxylin and eosin, cresyl violet, thioflavin S, or Congo red stains, or by using the Bielschowsky silver methods.

For immunohistologic studies, endogenous peroxidase was quenched by treatment with 6% hydrogen peroxide in methanol or with 3.0% hydrogen peroxide in methanol (1:5). To enhance APP antigen detection, selected sections were microwave irradiated in water at full power for 15 min, cooled to room temperature, transferred to deionized water in 0.5 M TBS (pH 7.6), and pretreated with 0.4% Triton X-100 in TBS (TX/TBS), followed by 3% normal goat serum in TBS. Primary antibodies 6E10 (1:100) and 8E5 (1:100 ascites fluid) were prepared in 0.1% TX/TBS with 2% normal goat serum. Following incubation for 24 hr, slides were incubated in goat anti-rabbit or anti-mouse IgG (1:20) in 0.1% TX/TBS, followed by a 1 hr incubation in rabbit or mouse peroxidase-antiperoxidase (1:100) at room temperature. Rinsed slides were reacted in the presence of 0.05% diaminobenzidine in 0.01% hydrogen peroxide. Representative sections were silver enhanced according to the Fontana–Masson method (Masson, 1928). Other sections were immersed in 70% formic acid for 10 min, rinsed in PBS, and immersed in 10% normal horse serum for 1 hr. Following incubation overnight at 4°C with primary antibody 6E10 (1:5000), sections were rinsed in PBS and incubated with anti-mouse IgG, followed by avidin-biotin complex (Vector Labs, Inc). Rinsed slides were reacted with diaminobenzidine and counterstained with Harris hematoxylin. GFAP was detected using a monoclonal antibody to porcine GFAP (Sigma).

Regional Brain Glucose Utilization Analysis

Mice received an intraperitoneal injection of [^{14}C]2-deoxyglucose (New England Nuclear; 5 μCi in 0.4 ml of 0.9% NaCl) and were sacrificed 60 min later. Brains were rapidly removed and frozen in isopentane cooled to −30°C with dry ice. A sample of trunk blood was collected and used for determination of plasma glucose concentration by a glucose analyzer (Beckman). Techniques for quantitative autoradiography have been described in detail previously (Iadecola et al., 1983; Iadecola and Xu, 1994) and are only summarized. Coronal brain sections (20 μm) were cut on a cryostat (Hacker-Bright), mounted on glass slides, and apposed to X-ray film (Dupont) together with calibrated ^{14}C standards (Iadecola et al., 1983). The film was developed 10 days later using an automatic developer (Kodak), and the optical density (OD) of regions of interest was determined bilaterally on four adjacent sections using a computerized image analyzer (MCID system, Imaging Research Inc.). OD was transformed into ^{14}C concentration (nCi/g) using the standards on the film. Owing to the small size of some mice (15–20 g), blood sampling for determination of the 2-deoxyglucose arterial time course could not be perfomed, except at the time of sacrifice. Therefore, a CGU index was obtained by dividing regional radioactivity values (nCi/100 g/min) by the radioactivity of a region devoid of pathology, the whole cerebellum. This normalization procedure has been validated and widely used in small laboratory animals (e.g., Sharp et al., 1983; Mitchell and Crossman, 1984; Williot et al., 1988). In our experiments, the rate of ^{14}C accumulation in cerebellum (nCi/100 g/min) and plasma glucose did not differ between control, aged, and transgenic mice. This finding indicates that the CGU index provides an accurate estimate of glucose utilization as determined by the method of Sokoloff et al. (1977).

Acknowledgments

All correspondence should be addressed to K. K. H. The authors wish to thank Stanley B. Prusiner and Mike Scott for the hamster PrP cosmid vector; Robert Ehlenfeldt and Dallas Foster for generating transgenic mice; Jane Diedrich for valuable help and advice; Sangram Sisodia for providing APP cDNAs; Steven Nilsen, Jennifer Loh, Jim Meiners, Michael Guarnieri, and John Mojekwu for technical assistance; and David Knopman and Richard Price for support and encouragement. This work was supported by grants from the National Institutes of Health (AG07914, AG05146, and NS20471 to D. P. and D. R. B.; AG10681 to G. C.; and NS33249 to K. H.), the Alzheimer's Association (K. K. H. and D. R. B.), the Culpeper Foundation (K. K. H.), and the Neurosciences Education and Research Foundation (K. K. H.).

The costs of publication of this article were defrayed in part by the payment of page charges. This article must therefore be hereby marked *"advertisement"* in accordance with 18 USC Section 1734 solely to indicate this fact.

Received July 19, 1995; revised September 14, 1995.

References

Araki, W., Kunishita, T., Takahashi, K., Ikeda, S., and Tabira, T. (1994). Demonstration of amyloid β-protein secretion in a mouse neuronal cell line. Neurosci. Lett. *167*, 125–127.

Arriagada, P.V., Marzloff, K., and Hyman, B.T. (1992). Distribution of Alzheimer-type pathologic changes in nondemented elderly individuals matches the pattern in Alzheimer's disease. Neurology *42*, 1681–1688.

Baribault, H., Penner, J., Iozzo, R., and Wilson-Heiner, M. (1994). Colorectal hyperplasia and inflammation in keratin 8-deficient FVB/N mice. Genes Dev. *8*, 2964–2973

Braak, H., and Braak, E. (1991). Neuropathological staging of Alzheimer-related changes. Acta Neuropathol. *82*, 239–259.

Buxbaum, J.D., Christensen, J.L., Ruefli, A.A., Greengard, P., and Loring, J.F. (1993). Expression of APP in brain of transgenic mice containing the entire human APP gene. Biochem. Biophys. Res. Commun. *197*, 639–645.

Cai, X.-D., Golde, T.E., and Younkin, S.G. (1993). Release of excess amyloid β protein from a mutant amyloid β protein precursor. Science *259*, 514–516.

Chartier-Harlin, M.-C., Crawford, F., Houlden, H., Warren, A., Hughes, D., Fidani, L., Goate, A., Rossor, M., Roques, P., Hardy, J., and Mullan, M. (1991). Early-onset Alzheimer's disease caused by mutation at codon 717 of the β-amyloid precursor protein gene. Nature *353*, 844–846.

Citron, M., Oltersdorf, T., Haass, C., McConlogue, L., Hung, A.Y., Seubert, P., Vigo, P.C., Lieberburg, I., and Selkoe, D.J. (1992). Mutation of the β-amyloid precursor protein in familial Alzheimer's disease increases β-protein production. Nature *360*, 672–674.

Corder, E.H., Saunders, A.M., Strittmatter, W.J., Schmechel, D.E., Gaskell, P.C., Small, G.W., Roses, A.D., Haines, J.L., and Pericak, V.M.A. (1993). Gene dose of apolipoprotein E type 4 allele and the risk of Alzheimer's disease in late onset families. Science *261*, 921–923.

Crystal, H., Dickson, D., Fuld, P., Masur, D., Scott, R., Mehler, M., Masdeu, J., Kawas, C., Aronson, M., and Wolfson, L. (1988). Clinico-pathologic studies in dementia: nondemented subjects with pathologically confirmed Alzheimer's disease. Neurology *38*, 1682–1687.

de Leon, M.J., Ferris, S.H., George, A.E., Christman, D.R., Fowler, J.S., Gentes, C., Reisberg, B., Gee, B., Emmerich, M., Yonekura, et al. (1983). Positron emission tomography studies of aging and Alzheimer's disease. Am. J. Neuroradiol. *4*, 568–571.

Douglas, R.J. (1990). Spontaneous alternation behavior and the brain. In Spontaneous Alternation Behavior, W. N. Denber and L. L. Richman, eds. (New York: Springer-Verlag), pp. 73–109.

Evans, D.A., Funkenstein, H.H., Albert, M.S., Sherr, P.A., Cook, N.R., Chown, M.J., Hebert, L.E., Hennekens, C.H., and Taylor, J.O. (1989).

Prevalence of Alzheimer's disease in a community population of older persons: higher than previously reported. J. Am. Med. Assoc. *262*, 2551–2556.

Finch, C. (1993). Neuron atrophy during aging: programmed or sporadic? Trends Neurosci. *16*, 104–110.

Gage, F.H., Kelly, P.A.T., and Björklund, A. (1984). Regional changes in brain glucose metabolism reflect cognitive impairments in aged rats. J. Neurosci. *11*, 2856–2865.

Games, D., Adams, D., Alessandrini, R., Barbour, R., Berthelotte, P., Blackwell, C., Carr, T., Clemens, J., Donaldson, T., Gillespie, F., et al. (1995). Alzheimer-type neuropathology in transgenic mice overexpressing V717F β-amyloid precursor protein. Nature *373*, 523–527.

Gerlai, R., Marks, A., and Roder, J. (1994). T-maze spontaneous alternation rate is decreased in S100β transgenic mice. Behav. Neurosci. *108*, 100–106.

Goate, A.M., Chartier-Harlin, C.M., Mullan, M., Brown, J., Crawford, F., Fidani, L., Giuffra, L., Haynes, A., Irving, N., James, L., et al. (1991). Segregation of a missense mutation in the amyloid precursor protein gene with familial Alzheimer's disease. Nature *349*, 704–706.

Gravina, S.A., Ho, L., Eckman, C.B., Long, K.E., Otvos, L., Younkin, L.H., Suzuki, N., and Younkin, S.G. (1995). Amyloid β protein (Aβ) in Alzheimer's disease brain. Biochemical and immunocytochemical analysis with antibodies specific for forms ending at $A\beta_{40}$ or $A\beta_{42(43)}$. J. Biol. Chem. *270*, 7013–7016.

Hanley, T., and Merlie, J.P. (1991). Transgene detection in unpurified mouse tail DNA by polymerase chain reaction. Biotechniques *10*, 56.

Hendriks, L., Duijn, C.M. v., Cras, P., Cruts, M., Hul, W.V., Harskamp, F. v., Warren, A., McInnis, M.G., Antonarakis, S.E., Martin, J.-J., et al. (1992). Presenile dementia and cerebral hemorrhage linked to a mutation at codon 692 of the β-amyloid precursor protein gene. Nature Genet. *1*, 218–221.

Higgins, L.S., Holtzman, D.M., Rabin, J., Mobley, W.C., and Cordell, B. (1994). Transgenic mouse brain histopathology resembles early Alzheimer's disease. Ann. Neurol. *35*, 598–607.

Hogan, B.F., Constantini, F., and Lacy, E. (1986). Manipulating the Mouse Embryo: A Laboratory Manual (New York: Cold Spring Harbor Laboratory Press).

Hsiao, K.K., Scott, M., Foster, D., Groth, D.F., DeArmond, S.J., and Prusiner, S.B. (1990). Spontaneous neurodegeneration in transgenic mice with mutant prion protein. Science *250*, 1587–1590.

Hsiao, K.K., Groth, D., Scott, M., Yang, S.-L., Serban, H., Raff, D., Foster, D., Torchia, M., DeArmond, S.J., and Prusiner, S.B. (1994). Serial transmission in rodents of neurodegeneration from transgenic mice expressing mutant prion protein. Proc. Natl. Acad. Sci. USA *91*, 9126–9130.

Iadecola, C., Nakai, M., Mraovitch, S., Ruggiero, D.A., Tucker, L.W., and Reis, D.J. (1983). Global increase in cerebral metabolism and blood flow produced by focal electrical stimulation of dorsal medullary reticular formation in rat. Brain Res. *272*, 101–114.

Iadecola, C., and Xu, X. (1994) Nitro—arginine attenuates hypercapinic cerebrovasodilation without affecting cerebral metabolism. Am. J. Physiol. *266*, R518–R525.

Kammesheidt, A., Boyce, F.M., Spanoyannis, A.F., Cummings, B.J., Ortegon, M., Cotman, C., Vaught, J.L., and Neve, R.L. (1992). Deposition of β/A4 immunoreactivity and neuronal pathology in transgenic mice expressing the carboxyl-terminal fragment of the Alzheimer amyloid precursor in the brain. Proc. Natl. Acad. Sci. USA *89*, 10857–10861.

Kim, K.S., Wen, G.Y., Bancher, C., Chen, C.M.J., Sapienze, V.J., Hong, H., and Wisniewwski, H.M. (1990). Detection and quantitation of amyloid β-peptide with 2 monoclonal antibodies. Neurosci. Res. Commun. *7*, 113–122.

Kinney, H.C., and Sidman, R.L. (1986). Pathology of the spongiform encephalopathy in the grey tremor mutant mouse. J. Neuropathol. Exp. Neurol. *45*, 108–126.

Kokmen, E., Beard, C.M., Offord, K.P., and Kurland, L.T. (1989). Prevalence of medically diagnosed dementia in a defined United States population: Rochester, Minnesota, January 1, 1975. Neurology *39*, 773–776.

Kumar, A, Schapiro, M.B., Grady, C., Haxby, J.V., Wagner, E., Salerno, J.A., Friedland, R.P., and Rapoport, S.I. (1991). High resolution PET studies in Alzheimer's disease. Neuropsychopharmacology *4*, 35–45.

Laemmli, U.K. (1970). Cleavage of structural proteins during the assembly of the head of bacteriophage T4. Nature *227*, 680–685.

LaFerla, F.M., Tinkle, B.T., Bieberich, C.J., Haudenschild, C.C., and Jay, G. (1995). The Alzheimer's Aβ peptide induces neurodegeneration and apoptotic cell death in transgenic mice. Nature Genet. *9*, 21–30.

Lamb, B.T., Sisodia, S.S., Lawler, A.M., Slunt, H.H., Kitt, C.A., Kearns, W.G., Pearson, P.L., Price, D.L., and Gearhart, J.D. (1993). Introduction and expression of the 400 kilobase *precursor amyloid protein* gene in transgenic mice. Nature Genet. *5*, 22–30.

Landfield, P., Rose, G., Sandles, L., Wohlstadter, T.C., and Lynch, G. (1977). Patterns of astroglial hypertrophy and neuronal degeneration in the hippocampus of aged, memory-deficient rats. J. Gerontol. *32*, 3–12.

Levy-Lehad, E., Wasco, W., Poorkaj, P., Romano, D.M., Oshima, J., Pettingell, W.H., Yu, C., Jondro, P.D., Schmidt, S.D., Wang, K., et al. (1995). Candidate gene for the chromosome 1 familial Alzheimer's disease locus. Science *269*, 973–977.

Masson, P. (1928). Carcinomas and nerve hyperplasia of the appendicular mucosa. Am. J. Pathol. *4*, 181–221.

Mitchell, I.J., and Crossman, A.R. (1984). In defense of optical density ratios in 2-deoxyglucose autoradiography. Brain Res. *298*, 191–192.

Moran, P.M., Higgins, L.S., Cordell, B., and Moser, P.C. (1995). Age-related learning deficits in transgenic mice expressing the 751-amino acid isoform of human β-amyloid precursor protein. Proc. Natl. Acad. Sci. USA *92*, 5341–5345.

Morris, R. (1984). Development of a water-maze procedure for studying spatial learning in the rat. J. Neurosci. Meth. *11*, 47.

Mullan, M., Crawford, F., Axelman, K., Houlden, H., Lilius, L., Winblad, B., and Lannfelt, L. (1992). A pathogenic mutation for probable Alzheimer's disease in the APP gene at the N-terminus of β-amyloid. Nature Genet. *1*, 345–347.

Murrell, J., Farlow, M., Ghetti, B., and Benson, M.D. (1991). A mutation in the amyloid precursor protein associated with hereditary Alzheimer's disease. Science *254*, 97–99.

Pearson, B.E., and Choi, T.K. (1993). Expression of the human β-amyloid precursor protein gene from a yeast artificial chromosome in transgenic mice. Proc. Natl. Acad. Sci. USA *90*, 10578–10582.

Prusiner, S.B., and Hsiao, K.K. (1994). Human prion diseases. Ann. Neurol. *35*, 385–395.

Prusiner, S.B., Scott, M., Foster, D., Pan, K.M., Groth, D., Mirenda, C., Torchia, M., Yang, S.L., Serban, D., and Carlson, G.A., et al. (1990). Transgenetic studies implicate interactions between homologous PrP isoforms in scrapie prion replication. Cell *63*, 673–686.

Quon, D., Wang, Y., Catalano, R., Scardina, J.M., Murakami, K., and Cordell, B. (1991). Formation of β-amyloid protein deposits in brains of transgenic mice. Nature *352*, 239–241.

Sandhu, F.A., Salim, M., and Zain, S.B. (1991). Expression of the human β-amyloid protein of Alzheimer's disease specifically in the brains of transgenic mice. J. Biol. Chem. *266*, 21331–21334.

Scott, M., Foster, D., Mirenda, C., Serban, D., Coufal, F., Walchli, M., Torchia, M., Groth, D., Carlson, G., DeArmond, S.J., et al. (1989). Transgenic mice expressing hamster prion protein produce species-specific scrapie infectivity and amyloid plaques. Cell *59*, 847–857.

Scott, M.R., Kohler, R., Foster, D., and Prusiner, S.B. (1992). Chimeric prion protein expression in cultured cells and transgenic mice. Prot. Sci. *1*, 986–997.

Sharp, F.R., Kilduff, T.S., Bzorgchami, S., Heller, H.C., and Ryan, A.F. (1983). The relationship of local cerebral glucose utilization to optical density ratios. Brain Res. *263*, 97–103.

Sherrington, R., Rogaev, E.I., Liang, Y., Rogaeva, E.A., Levesque, G., Ikeda, M., Chi, H., Lin, C., Li, G., Holman, K., et al. (1995). Cloning

of a gene bearing missense mutations in early-onset familial Alzheimer's disease. Nature *375*, 754–760.

Simpson, I.A., Chundu, K.R., Davies-Hill, T., Honer, W.G., and Davies, P. (1994). Decreased concentrations of GLUT1 and GLUT3 glucose transporters in the brains of patients with Alzheimer's disease. Ann. Neurol. *35*, 546–551.

Slunt, H.H., Thinakaran, G., Van Koch, C., Lo, A.C., Tanzi, R.E., and Sisodia, S.S. (1994). Expression of a ubiquitous, cross-reactive homologue of the mouse β-amyloid precursor protein (APP). J. Biol. Chem. *269*, 2637–2644.

Sokoloff, L., Reivich, M., Kennedy, C., Rosiers, M.H.D., Patlak, C.S., Pettigrew, K.D., Sakurada, O., and Shinohara, M. (1977). The ^{14}C-deoxyglucose method for the measurement of local cerebral glucose utilization: theory, procedure, and normal values in the conscious and anesthetized albino rat. J. Neurochem. *28*, 897–916.

Suzuki, N., Cheung, T.T., Cai, X.D., Okada, A.L., Otvos, J., Eckman, C., Golde, T.E., and Younkin, S.G. (1994). An increased percentage of long amyloid β protein secreted by familial amyloid β protein precursor (βAPP717) mutants. Science *264*, 1335–1340.

Taketo, M., Schroeder, A.C., Mobraaten, L.E., Gunning, K.B., Hanten, G., Fox, R.R., Roderick, T.H., Stewart, C.L., Lilly, F., Hansen, C. T, and Overbeek, P.A. (1991). FVB/N: an inbred mouse strain preferable for transgenic analyses. Proc. Natl. Acad. Sci. USA *88*, 2065–2069.

Telling, G., Scott, M., Hsiao, K., Foster, D., Yang, S.-L., Torchia, M., Sidle, K., Collinge, J., DeArmond, S., and Prusiner, S.B. (1994). Transmission of Cretuzfeldt–Jakob disease from humans to transgenic mice expressing chimeric human-mouse prion protein. Proc. Natl. Acad. Sci. USA *91*, 9936–9940.

Weidemann, A., Konig, G., Bunke, D., Fischer, P., Salbaum, J.M., Masters, C.L., and Beyreuther, K. (1989). Identification, biogenesis, and localization of precursors of Alzheimer's disease A4 amyloid protein. Cell *57*, 115–126.

Westaway, D., DeArmond, S.J., Cayetano-Canlas, J., Groth, D., Foster, D., Yang, S.-L., Torchia, M., Carlson, G.A., and Prusiner, S.B. (1994). Degeneration of skeletal muscle, peripheral nerves, and the central nervous system in transgenic mice overexpressing wild-type prion proteins. Cell *76*, 117–129.

Williot, J.F., Paris Hunter, K., and Coleman, J.R. (1988). Aging and presbycusis: effects on 2-deoxyglucose uptake in the mouse auditory brain stem in quiet. Exp. Neurol. *99*, 615–621.

Wong, P.C., and Cleveland, D.W. (1990). Characterization of dominant and recessive assembly-defective mutations in mouse neurofilament NF-M. J. Cell Biol. *111*, 1987–2003.

Yamaguchi, F., Richards, S.J., Beyreuther, K., Salbaum, M., Carlson, G.A., and Dunnett, S.B. (1991). Transgenic mice for the amyloid precursor protein 695 isoform have impaired spatial memory. NeuroReport *2*, 781–784.